J. Marine Sci. Appl. (2017) 16: 237-242
DOI: 10.1007/s11804-017-1412-z

Galvanic Interactions of HE15 / MDN138 & HE15 / MDN250 Alloys in Natural Seawater

G. T. Parthiban[1], G. Subramanian[2*], K. Muthuraman[1] and P. Ramakrishna Rao[3]

1. CSIR-Central Electrochemical Research Institute, Karaikudi-630003, India
2. Offshore Platform & Marine Electrochemistry Centre, CSIR-CECRI Unit, Harbour Area, Tuticorin-628004, India
3. Defence Research Development Laboratory, Hyderabad-500058, India

Abstract: HE15 is a heat treatable high strength alloy with excellent machinability find wide applications in aerospace and defence industries. In view of their excellent mechanical properties, workability, machinability, heat treatment characteristics and good resistance to general and stress corrosion cracking, MDN138 & MDN250 have been widely used in petrochemical, nuclear and aerospace industries. The galvanic corrosion behaviour of the metal combinations HE15 / MDN138 and HE15 / MDN250, with 1:1 area ratio, has been studied in natural seawater using the open well facility of CECRI's Offshore Platform at Tuticorin for a year. The open circuit potentials of MDN138, MDN250 and HE15 of the individual metal, the galvanic potential and galvanic current of the couples HE15 / MDN138 and HE15 / MDN250 were periodically monitored throughout the study period. The calcareous deposits on MDN138 and MDN250 in galvanic contact with HE15 were analyzed using XRD. The electrochemical behaviors of MDN138, MDN250 and HE15 in seawater have been studied using an electrochemical work station. The surface characteristics of MDN138 and MDN250 in galvanic contact with HE15 have been examined with scanning electron microscope. The results of the study reveal that HE15 offered required amount of protection to MDN138 & MDN250.

Keywords: alloy, MDN138, MDN250, HE15, galvanic corrosion, natural seawater

Article ID: 1671-9433(2017)02-0237-06

1 Introduction

MDN250 is an 18% nickel, cobalt strengthened steel (C-type), with excellent mechanical properties, workability and heat treatment characteristics. It is weld able without preheat, in both the annealed and aged condition. The alloy is very tough, relatively soft (30/34 R_c), therefore, readily machined and formed. Typical applications for maraging include missile and rocket motor cases, landing and takeoff gear, munitions, aerospace, extrusion tooling, die casting, high performance shafting, gears and fasteners. MDN138 is a precipitation, age hardenable stainless steel. Its principal features are high transverse toughness, good resistance to general and stress corrosion cracking, high strength that is developed by a single low temperature heat treatment and best welded in the solution annealed condition (Liu, 2015). This alloy has been used in aircraft components such as landing gear and structural sections, valves, shafts, and components in the petrochemical and nuclear industries. HE15 is a family of aluminum group-2014A and heat treatable high strength alloy with excellent machinability, good hard anodizing capability and easily plated find wide applications in aerospace and defence industries. With light weight and high performance characteristics HE15 aluminium alloy has a wide range of mechanical and corrosion resistance properties (ASM, 1981; Hutchings and Unterweiser, 1981; Osorio *et al*., 2009) and hence acts as an important material in defence & aerospace applications. The rocket motor components, such as booster and sustainer motors are fabricated using HE15 aluminium alloy (Mohan Reddy *et al*., 1995, Kciuk and Tkaczyk, 2007). In the present study the galvanic corrosion behaviour of the metal combinations HE15 / MDN138 and HE15 / MDN250, with 1:1 area ratio has been studied in natural seawater using the open well facility of CECRI's Offshore Platform at Tuticorin for a year, which is first of its kind in the literature of Indian waters.

2 Materials and methods

2.1 Materials

The materials (HE15, MDN138 & MDN250) were supplied by Defence Research and Development Laboratory, Hyderabad. The composition of HE15 is Cu: 3.9%–5.0%, Ni: 0.1%, Si: 0.5%–0.9%, Mg: 0.2%–0.8%, Fe: 0.5%, Mn: 0.4%–1.2%, Cr: 0.1%, Zn: 0.25%, Ti: 0.15%, Zr & Ti: 0.2% and Al: balance. The composition of MDN138 is Al: 1.0%, C: 0.04%, Cr: 12.5%, Mn: 0.18%, Mo: 2.0%, Ni: 7.5%, N: 0.01%, P: 0.01%, Si: 0.1%, S: 0.007% and Fe: balance. The composition of MDN250 is Al: 0.07%, C: 0.03%, Cr: 0.5%, Mn: 0.10%, Mo: 4.6%, Ti: 0.3%, Ni: 17.5%, Co: 7.5%, Cu: 0.5%, P: 0.01%, Si: 0.1%, S: 0.008% and Fe: balance.

2.2 Specimen preparation and galvanic interaction study by natural seawater exposure

The coupons of HE15, MDN250 & MDN138 of size 75mm×50 mm×6 mm, were cut from the respective sheets,

Received date: 15-Jul-2016
Accepted date: 02-Nov-2016
Foundation item: Supported by Project Director, DRDL, Hyderabad, India (Project No. SSP 0709)
***Corresponding author Email:** cgscorr@yahoo.co.in

removed corrosion products using the recommended pickling solutions (ASTM International, 2011), mechanically polished with different grits silicon carbide metallurgical paper (180, 220, 400, and 600), cleaned and degreased with acetone and weighed to an accuracy of 10^{-4} g, and stored in desiccators until use. Galvanic contact between the coupons HE15 & MDN250 and HE15 & MDN138 was effected by PVC sheathed 320SWG copper wires and the contact points were sealed using marine epoxy to prevent crevice corrosion. The galvanically coupled coupons HE15 & MDN250 and HE15 & MDN138 were fixed on a wooden frame with grooving and immersed in the natural seawater at a water depth 2 m below the mean low tide level using the open well facility of CECRI's Offshore Platform at Tuticorin. Periodic monitoring of the open circuit potential of the coupons HE15, MDN250 & MDN138 and the mixed potentials of the galvanic couples HE15 / MDN250 and HE15 / MDN138, were made daily using a high impedance voltmeter (Tektronix, Model DMM155) with an SCE. The galvanic current of the couples HE15 / MDN250 and HE15 / MDN138 was monitored periodically using zero impedance ammeter. The field studies were terminated after 330 days and the digital images of the galvanically coupled coupons HE15 & MDN138, and HE15 & MDN250, were recorded, with biomass & corrosion products and after removing biomass & corrosion products. The gravimetric corrosion rates of HE15, MDN138 & MDN250 were calculated after removal of corrosion products using the recommended pickling solutions (ASTM International, 2011). The fouling organisms on the surfaces of the galvanically coupled coupons (HE15 & MDN138 and HE15 & MDN 250) were recorded and visual observations were made on the surfaces of coupons after removal of biomass & corrosion products. The extent of galvanic protection offered by HE15 to MDN138 & MDN250 has been calculated from the gravimetric corrosion rate values of both freely corroded and galvanically coupled MDN138, MDN250 & HE15.

2.3 Physicochemical characteristics of seawater

Subsurface seawater was collected from the test location on a quarterly basis during the 12 months study period using a Hydro-Bios (Kiel) water sampler. Analyses were carried out following the standard procedures outlined by Strickland and Parsons (1972) which included general physico-chemical parameters, dissolved nutrients and major ions. Heavy metals in the water samples were extracted following APDC-MIBK pre-concentration procedure (Brooks *et al.*, 1967) and estimated on an atomic absorption spectrometer (GBC 932 Plus).

2.4 Characterization of calcareous deposits on MDN138 & MDN250

The galvanic coupled coupons of MDN138 & MDN250 after retrieval from seawater were washed with double distilled water and dried. The calcareous deposits on MDN138 & MDN250 were analyzed using XRD (X'pert PRO PAN analytical diffractometer with Syn master 793^s, Netherlands).

2.5 Surface characterization of MDN138 & MDN250

The fouling assemblage on the galvanic coupled coupons of MDN138 & MDN250 after retrieval from seawater was scraped and the corrosion products were removed using the recommended pickling solutions (ASTM International, 2011), washed in distilled water anddried. The surface morphology of the coupons were examined under the Scanning Electron Microscope (SEM) (HITACHI Model S-3000H instruments).

2.6 Electrochemical behaviour HE15, MDN250 & MDN138 in natural seawater

The potentiodynamic polarization curves of HE15, MDN138 & MDN250 were drawn by conducting experiments separately for HE15, MDN138 and MDN250, using AUTOLAB PGSTAT30 in the feed potential range of −1 000 mV to 1 000 mV with 3 electrodes cell arrangement with HE15 / MDN138 / MDN250 as working electrode, Ag/AgCl as reference electrode and platinum as counter electrode in natural seawater.

3 Results and discussion

The mean values of physicochemical parameters of seawater of Open sea-Tuticorin are presented in Table 1. In general the values of the water quality parameters were found to be normal, and did not show much seasonal variation during the study period. Hence the mean values of the four quarters are taken for consideration. Fig. 1 portrays the open circuit potential values of HE15 & MDN250 and the mixed potential values of the couple HE15 / MDN250 and Fig. 2 portrays the open circuit potential values of HE15 & MDN138 and the mixed potential values of the couple HE15 / MDN138, recorded throughout the study period. The galvanic current values of the galvanic couples HE15 / MDN250 and HE15 / MDN138, recorded throughout the study period are given in Fig. 3.

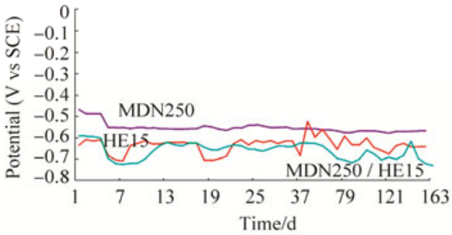

Fig. 1 Open circuit potential and mixed potential of HE15 & MDN250

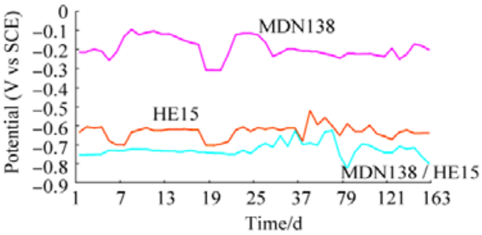

Fig. 2 Open circuit potential and mixed potential of HE15 & MDN138

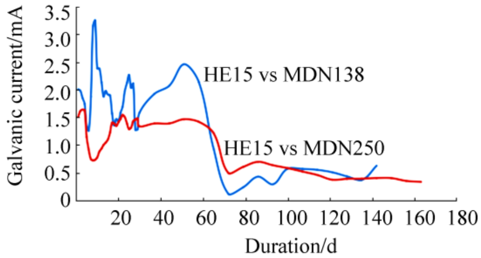

Fig. 3 Galvanic current values of the couples HE15 / MDN138 & HE15 / MDN250

Table 1 Seawater quality parameters of the Open sea-Tuticorin showing the mean values (*n*=4) and their SDs

Parameters	Open sea-Tuticorin	
	Mean	Standard deviation
Salinity/ ‰	35.00	0.74
pH	8.1	0.113 389
Dissolved Oxygen/(ml·L^{-1})	4.85	0.265 922
Inorganic Phosphate/(μmol·L^{-1})	0.725	0.074 066
Total Phosphorous/(μmol·L^{-1})	3.27	1.195 894
Nitrite/(μmol·L^{-1})	0.017	0.000 983
Nitrate/(μmol·L^{-1})	4.37	0.297
Silicate/(μmol·L^{-1})	18.83	2.76
Ammonia/(μmol·L^{-1})	2.25	0.134 164
Calcium/(mg·L^{-1})	400	19.820 6
Magnesium/(mg·L^{-1})	1275	97.247 84
Copper/(μg·L^{-1})	2.7	0.47
Cadmium/(μg·L^{-1})	1.30	0.217
Lead/(μg·L^{-1})	14	0.727 8
Iron/(μg·L^{-1})	54.0	15.928
Manganese/(μg·L^{-1})	5.50	0.790 569
Zinc/(μg·L^{-1})	1.570	0.594 7
Mercury/(μg·L^{-1})	1.196	0.234 379

3.1 Visual observations

3.1.1 HE15 / MDN138

Fig. 4 portrays the digital images of the surface of galvanically coupled HE15 & MDN138 after termination of the experiment. The surface of the galvanically coupled HE15 is characterized by barnacles with white corrosion products, while that of MDN138 is characterized predominantly by barnacles as primary foulers and fewer oysters. Fig. 5 portrays the digital images of the surface of galvanically coupled HE15 & MDN138 after removal of corrosion products and biomass. The surface of the galvanically coupled HE15 after removal of corrosion products and biomass is characterized by pits beneath passive corrosion products, whereas no characteristic pitting was observed on MDN138.

3.1.2 HE15 / MDN250

Fig. 6 portrays the digital images of the surface of galvanically coupled HE15 & MDN 250 after termination of the experiment. The surface of the galvanically coupled HE15 is characterized by barnacles with white corrosion products, while that of MDN250 is characterized by barnacles and oysters. Fig. 7 portrays the digital images of the surface of galvanically coupled HE15 & MDN250 after removal of corrosion products and biomass. The surface of the galvanically coupled HE15 after removal of corrosion products and biomass is characterized by pits beneath passive corrosion products, whereas no characteristic pitting was observed on MDN250.

Fig. 4 Surface of the galvanically coupled coupons of HE15 (Right) & MDN138 (Left) exposed in natural seawater for 330 days

Fig. 5 Surface of the galvanically coupled coupons of HE15 (bottom) & MDN138 (top) after removal of biomass and corrosion products

Fig. 6 Surface of the galvanically coupled coupons of HE15 (Right) & MDN250 (Left) exposed in natural seawater for 330 days

Fig. 7 Surface of the galvanically coupled coupons of HE15 (top) & MDN250 (bottom) after removal of biomass and corrosion products

3.2 Characterization of calcareous deposits on MDN138 & MDN250

The nature of calcareous deposits formed on the galvanically protected MDN138 & MDN250 as analyzed by XRD are found to be same and given in Fig. 8. The compounds were identified as $CaCO_3$ (calcite, aragonite and vaterite), $MgCO_3$ (magnesite), $Mg(OH)_2$ (brucite) and MgO (brucite). With particular reference to $CaCO_3$, more aragonite phases were recorded than calcite or vaterite.

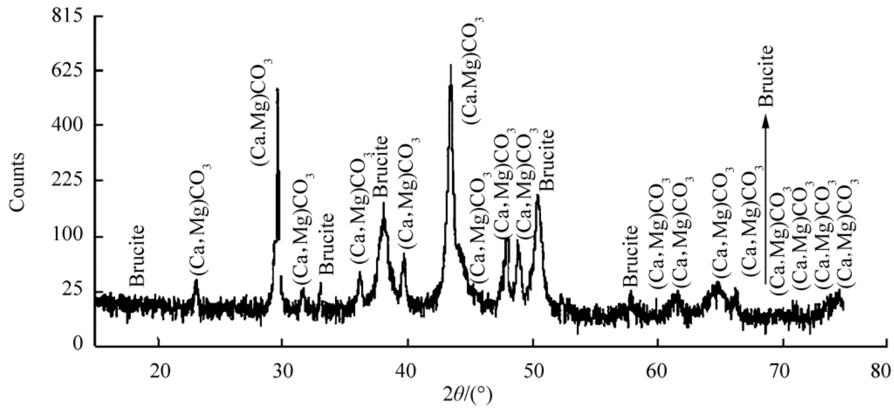

Fig. 8 XRD pattern of calcareous deposits formed on the surfaces of galvanically protected MDN138 & MDN250

3.3 Open circuit potential, galvanic potential & galvanic current

3.3.1 HE15 / MDN138

The OCP of MDN138 from the commencement (−0.217 V) of experiment had experienced many upward and downward surges during the study period, which is more pronounced up to 28th day and the fluctuation ranges between −0.312 V & −0.098 V. The OCP of HE15 from the commencement (−0.637 V to till the end of the experiment (−0.644 V) lies in the range between −0.709 & −0.524 V. Only minor fluctuations are observed. The galvanic potential values of the couple from the commencement (−0.756 V), experienced a plateau like curve up to 22nd day (−0.751 V) and from thereupon a number of undulations more in the upward direction & 1 or 2 in the downward direction, till the end (−0.803 V) of the experiment.

The galvanic current values of the couple between 6th day (1.262 mA) & 51st day (2.46 mA) experienced 3 undulations in the range between 3.25 mA & 1.28 mA, thereafter a steep decline up to 72nd day (0.12 mA). The steep increase in the galvanic current values from 7th day to 9th day could be attributed to the initial current demand for effective protection of the cathode surface until the formation of an adherent thin film of calcareous deposit. Cathodic protection alters the ionic concentration at the interface, increasing the hydroxyl ion concentration (Sarlak *et al*., 2009; Wieng *et al*., 2007). The consequent pH increase reduces the solubility of calcium, magnesium and bicarbonate ions at the interface favouring the precipitation of a calcareous scale according to the following reactions:

$$O_2 + 2H_2O + 4e^- \rightarrow 4\ OH^-$$
$$2H_2O + 2e^- \rightarrow 2OH^- + H_2$$
$$Ca^{2+} + CO_3^{2-} \rightarrow CaCO_3$$
$$HCO_3^- + OH^- \rightarrow H_2O + CO_3^{2-}$$
$$Mg^{2+} + 2OH^- \rightarrow Mg(OH)_2$$

A steady and gradual decline in the galvanic current values between 52nd day (2.46 mA) & 74th day (0.118 mA) has been observed. The upward surge of the current values between 79th day (0.239 mA) and 142nd day (0.627 mA) can be accounted owing to the impairment caused to the calcareous deposit film, by the combined effect of turbulence in the sea and settlement of fouling organisms on the cathodic surface (MDN138). Thus the onset of steady state current has been never attained till the end of the experiment. This is further evinced from the fact that the consumption of the HE15 which served as anode would be more. This has been further supported by the digital image of the surface of the coupon HE15 and visual observation after removal of biomass & corrosion products, characterized by numerous pits.

Despite the overwhelming evidence that bacteria and calcareous deposits coexist on cathodically protected surfaces, their interrelationships are not understood (Little and Wagner, 1993). The growth of calcareous deposits can interact in different ways with biofilms still present on the surfaces. Some bacteria can cause their dissolution. Some deposits can be disbanded from surfaces, and surface acidification can occur even under cathodic protection. Deposits lead to an increase of concentration polarization values and promote the effectiveness of cathodic protection. Porous deposits could become harmful with cathodic protection current blackout (Dexter and Lafontaine, 1989; Dickinson *et al*., 1996). The pattern of the curve infers that HE15 would have offered required amount of protection to MDN138. This has been further supported by the digital image of the surface of the coupon MDN138 and visual observation after removal of biomass & corrosion products.

3.3.2 HE15 / MDN 250

The OCP of MDN250 from the commencement (−0.468 V) of the experiment, experienced only minor fluctuations

(−0.553 to −0.568 V) throughout the study period. The OCP of HE15 from the commencement (−0.637 V to till the end of the experiment (−0.644 V) lies in the range between −0.709 & −0.524 V. Only minor fluctuations are observed. The galvanic potential of the couple from the commencement (−0.592 V) experienced 2 major downward shift undulations between 4th & 13th and 58th & 100th day, and minor undulations (6 Nos.) with upward shift.

Applying, Cathodic Protection (CP) to metallic surfaces in seawater causes the formation of calcareous deposit on cathodic surface owing to the precipitation of calcium and magnesium salts, such as calcite, aragonite and brucite. These deposits increase the throwing power of CP, decreasing the cathodic current demand and consequently the cost of CP. Both the chemical composition and structure of the deposit greatly influence the effectiveness of CP. Many parameters affect this deposition, including flow velocity (Lee and Ambrose, 1986; Hack and Guanti, 1989), the calcium and magnesium content of seawater (Culberson, 1983), temperature (Kunjapur *et al*., 1985), dissolved organic matter (Edyvean, 1987) and pressure. However, interfacial pH (Culberson, 1983) is the most significant factor and any factor which affects this can modify the deposition kinetics, along with the nature and the stability of the scale.

The galvanic current values of the couple experienced a deep fall between 4th (1.62 mA) & 8th (1.72 mA), thereafter a steep increase up to 22nd day (1.54 mA), from thereupon 2 minor undulations up to 58th day between the range 1.28 & 1.48 mA, and a steep downfall between 65th (1.21 mA) & 72nd day (0.49 mA); have been observed. The OCP of MDN250 from the commencement (−0.468 V) of the experiment, experienced only minor fluctuations (−0.553 to −0.568 V) throughout the study period. The galvanic potential of the couple HE15 / MDN250 from the commencement (−0.592 V) to till the end (−0.731 V) of the experiment lies in the range of −0.592 to −0.731 V. No major fluctuations are observed throughout the study period. Hence HE15 would have offered reasonable protection to MDN250. The pattern of the curve indicates HE15 would have offered complete protection to MDN250 during the entire study period.

3.3.3 Extent of galvanic protection offered by HE15 to MDN138 & MDN250

The numerous undulations in the galvanic current curve of the HE15 / MDN138, reveals that HE15 would have experienced more dissolution in order to offer protection to MDN138. Unlike HE15 of HE15/MDN138 couple, the HE15 of HE15 / MDN250 would have experienced less dissolution in order to offer complete protection to MDN250, in view of the less potential difference between HE15 & MDN250 and also the lesser undulations in the galvanic current curve of the couple HE15 / MDN250. The galvanic protection offered by HE15 to MDN138 and MDN 250 during the study period of 330 days amounts to 97% and 95%, respectively. This further reaffirms that the galvanic protection offered by HE15 is continuous and effective, which has been evinced from the adherent nature of the calcareous deposit film comprising compounds such as $CaCO_3$ (calcite, aragonite and vaterite), $MgCO_3$ (magnesite), $Mg(OH)_2$ (brucite) and MgO (brucite), despite the local disturbances by the combined effect of turbulence in the sea and settlement of fouling organisms on the cathodic surface (Subramanian *et al*., 2016).

3.4 Surface characteristics of MDN138 & MDN250 in galvanic contact with HE15

The surface morphology of the MDN 138 specimen in galvanic contact with HE15 reveals that no characteristic corrosion region could be observed and the whole surface has been covered by the uniform film of calcareous deposits, thus the entire surface has been well protected throughout the study period (Fig. 9). Likewise the surface morphology of the MDN250 specimen in galvanic contact with HE15 reveals that no characteristic corrosion region could be observed and the whole surface has been covered by the uniform film of calcareous deposits, thus the entire surface has been well protected throughout the study period. The signs of minute white spots on the MDN250 would be accounted for the partly unremoved particles of calcareous film even after cleaning in pickling solution.

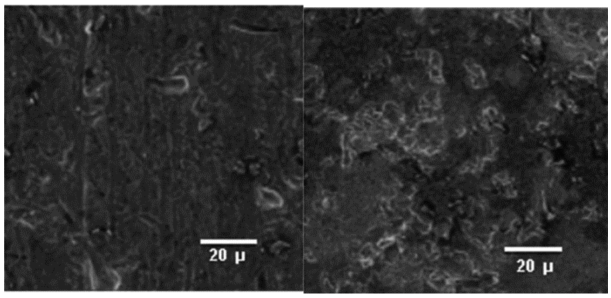

(a) MDN138 (b) MDN250

Fig. 9 Surface morphology of the galvanically protected MDN138 and MDN250

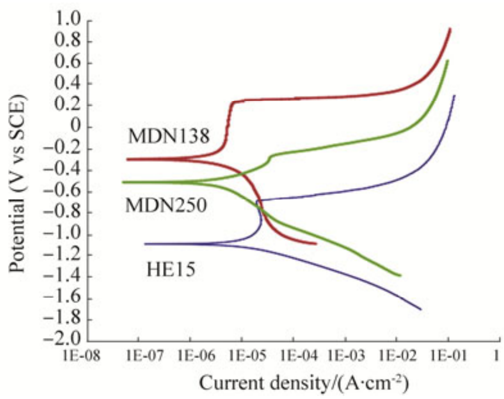

Fig. 10 Potentiodynamic polarization curves of HE15, MDN250 & MDN138

3.5 Potentiodynamic polarization scans of HE15, MDN138 & MDN250

Potentiodynamic polarization scans of freely corroded HE15, MDN138 & MDN250 in natural seawater reveal the characteristic nature of the individual metal and the trend corroborates with open circuit potential values of the individual metal (Fig. 10). The current density values are in the order of HE15> MDN250> MDN138. Hence, among MDN250 & MDN138, the MDN138 alloy is more corrosion resistant (Liu, 2015, Subramanian *et al*., 2016).

4 Conclusions

The galvanic protection offered by HE15 to MDN138 and MDN250 in natural seawater amounts to 97% and 95%, respectively, revealing that the galvanic protection offered by HE15 is continuous and effective, which has been further evinced from the adherent nature of the calcareous deposit film comprising compounds such as $CaCO_3$ (calcite, aragonite and vaterite), $MgCO_3$ (magnesite), $Mg(OH)_2$ (brucite) and MgO (brucite), despite the local disturbances by the combined effect of turbulence in the sea and settlement of fouling organisms on the cathodic surface. The surface morphologies of MDN138 & MDN250 reveal that no characteristic corrosion spot imply the extent of protection offered by HE15. Electrochemical polarization study reveals that MDN138 alloy is more corrosion resistant than MDN250 alloy.

Acknowledgement

The authors wish to thank the Director, The CSIR-Central Electrochemical Research Institute, Karaikudi, for permission and encouragements.

References

ASTM International, 2011. *Standard practice for preparing, cleaning, and evaluating corrosion test coupons*. ASTM standards, ASTM International, West Conshohocken, Designation G1-03.

Brooks RR, Presley BJ, Kaplan IR, 1967. APDC-MIBK extraction system for the determination of trace elements in saline waters by atomic absorption. *Talanta*, **14**(7), 806-816. DOI: 10.1016/0039-9140(67)80102-4

Culberson CH, 1983. Effect of seawater chemistry on the formation of calcareous deposits. *Corrosion 1983*, Houston, Paper No. 61.

Dexter SC, Lafontaine JP, 1989. Effect of natural marine biofilms of galvanic corrosion. *Corrosion*, **54**(11), 851-861.

Dickinson WH, Caccavo F, Lewandowski Z, 1996. The ennoblement of stainless steel by manganic oxide biofilms. *Corrosion Science*, **38**(8), 1407-1422. DOI: 10.1016/0039-9140(67)80102-4

Edyvean RGJ, 1987. Interactios between microfouling and the calcareous deposit formd on cathodically protected steel in seawater. *6th Intl Cong Marine Corrosion and Fouling*, Vol: Marine Biology, Athens, 469-475.

Hack HP, Guanti RJ, 1989. Effect of high flow on calcareous deposits and cathodic protection current density. *Materials Performance*, **28**(3), 29-35.

ASM, 1981. Exfoliation corrosion of HE.15 aluminium alloy. In *Failure analysis: The British Engine Technical Reports*, F.R. Hutchings and P.M. Unterweiser Ed., American Society for Metals.

Hutchings FR, Unterweiser PM, 1981. Exfoliation corrosion of HE.15 aluminium alloy. In *Failure analysis: The British Engine Technical Reports*, American Society for Metals.

Kciuk M, Tkaczyk S, 2007. Structure, mechanical properties and corrosion resistance of AlMg5 and AlMg1Si1 alloys. *Journal of Achievements in Materials and Manufacturing Engineering*, **21**(1), 39-42.

Kunjapur M, Hartt W, Smith S, 1985. Influence of temperature on calcareous deposition cathodically polarized steel in seawater. *Corrosion 1985*, Houston, Paper No. 316.

Lee R, Ambrose J, 1986. A hydrodynamical and chemical study of calcareous deposits. *Corrosion 1986*, Houston, Paper No. 292.

Little BJ, Wagner PA, 1993. The interrelationship between marine biofouling and cathodic protection. *Corrosion 1993*, Houston, Paper No. 525.

Liu H, 2015. Mechanical properties and corrosion behaviors of novel Cr2Ni Low-alloy construction steel. *International Journal of Electrochemical Science*, **10**(3), 2130-2140

Mohan Reddy T, Subanandha Rao A, Sambasiva Rao M, 1995. Design and development of propulsion system for antitank guided missile. *Defence Science Journal*, **45**(3), 213-219. DOI: 10.14429/dsj.45.4121

Osorio RW, Noe C, Peixoto CL, Amauri G, 2009. Corrosion resistance and mechanical properties of an Al 9wt% Si alloy treated by laser surface remelting. *International Journal of Electrochemical Science*, **4**(6), 820-831.

Sarlak M, Shahrabi T, Zamanzade M, 2009. Investigation of calcareous deposits formation on copper and 316L stainless steel under cathodic polarization in artificial seawater. *Protection of Metals and Physical Chemistry of Surfaces*, **45**(2), 216-222. DOI: 10.1134/S2070205109020166

Strickland JDH, Parsons TR 1972. *A practical handbook of seawater analysis*. Fisheries Research Board of Canada, Ottawa, 310.

Subramanian G, Parthiban GT, Muthuraman K, Ramakrishna rao P, 2016. Galvanic corrosion behaviour of HE20/MDN138 & HE20/MDN 250 alloys in natural seawater. *Journal of Marine Science and Application*, **15**(3), 343-348. DOI: 10.1007/s11804-016-1375-5

Wieng SM, Osvoll H, Gartland PO, 2007. Efficient cathodic protection to stainless steel small bore tubing. *Corrosion 2007*, Houston, Paper No. 07078.